A PHASED CHOPPER AT WNR**

by

V. Bolie*, R.M. Brugger+, R. N. Silver
Physics Division
Los Alamos National Laboratory
Los Alamos, NM 87545

ABSTRACT

At WNR, a proportional-integral-derivative PID control system has been developed to hold a neutron chopper within the 128 μsec wide window allowed by LAMPF. After achieving this control, LAMPF is triggered from the chopper to limit the phase jitter between the LAMPF produced burst of neutrons and the chopper opening. This PID system has been tested for phase control, phase jitter and neutron control using a chopper spinning at 14,400 RPM. The results to date, which are discussed, indicate that a chopper can be phased to the neutron pulses produced by LAMPF to $\pm$ 0.5 μsec..

*Permanent address: Department of Electrical and Computer Engineering
University of New Mexico
Albuquerque, NM

+Permanent address: University of Missouri Research Reactor
University of Missouri
Columbia, MO

** A paper presented at the VIth annual ICANS Meeting, ANL, June 28, 1982.

I. Introduction

Since the beginning of slow neutron spectroscropy, phased chopper-velocity selectors[1,2] have been important instruments for inelastic neutron scattering experiments. With the advent of the new pulsed spallation neutron sources, a chopper phased to the pulsed source [3,4,5,6] is again projected to be an important spectrometer. At the WNR pulsed source, the LAMPF proton accelerator produces the neutron bursts in phase with the 60 Hz wave form of the commercial power-line voltage. Since the power line frequency is not exact, it is a challenge to keep a chopper, with its required high moment of inertia, sufficiently in phase ($\pm$ 1/2 μsec) with the neutron bursts to achieve precise time-of-flight TOF resolution. Unfortunately, this problem will remain after completion of the Proton Storage Ring, PSR. Despite the PSR's anticipated capability to store protons for extraction, maximum current will be achieved by minimizing storage time to minimize beam spill. This paper presents the recent success in developing a control system for chopper phasing at the WNR. A discussion of the effort to solve a similar problem at the SNS at the Rutherford Laboratory was presented at the ICANS IV meeting.[8]

II. Statement of the Problem

Fig. 1 shows a schematic layout of the coupling of the LAMPF accelerator to a chopper at the WNR. With the switch U in the down position, LAMPF is triggered directly by the zero crossings of the commercial power line. The accelerator delivers proton bursts to a spallation target at the WNR to produce neutron bursts. To define the incident energy of the neutron beam impinging on the sample, the chopper must open at a fixed time delay after the neutron burst. To maintain this delay, a control system is required. Because the chopper mass, and hence moment of inertia, must be large in order for the chopper to be neutronically effective, it is impractical to control the phase of the chopper to the required accuracy of $\pm$ 1/2 μsec alignment with the zero crossings of the power-line voltage. Therefore, LAMPF allows a 128 μsec wide window around each zero

crossing of the line voltage during which a signal from one chopper at WNR can be sent to LAMPF to trigger the accelerator. This requires the switch U to be in the up position. The first challenge, then, is to maintain the chopper phase alignment to within + 64μsec of the power line phase.

Characteristics of the power line are shown in Figs. 2 and 3. A typical plot of the deviation of the period from 1/60 Hz is shown as a function of time in Fig. 2. Each point has been averaged over 10 seconds. One notes that there are long term trends as well as a great deal of statistical scatter. Similar behavior occurs regardless of the scale, even down to seconds. The limitation for control purposes is determined by the short time behavior. Fig. 3 is a plot of the autocorrelation function of the period as a function of time. There is above the top of the graph a white noise spike at zero time. The curve shows a characteristic time scale for the fall off of correlations of about 10 seconds. The power spectral density of the period deviations may be approximately represented by

$$(1)\quad \frac{d\sigma^2}{d\nu} = \frac{\sigma_1^2}{2\nu_1} \exp\left(-|\nu|/\nu_1\right)$$

with $\sigma_1 \simeq .011$ Hz and $\nu_1 \simeq .025$ Hz.

Consider a proportional-integral-derivative PID control system in which the feedback torque is applied to the chopper is a sum of terms proportional to the phase error, to its integral, and to its derivative. Then, ignoring the integral term,

$$(2)\quad JN\ddot{\varepsilon} + C\dot{\varepsilon} + K\varepsilon = JN\ddot{\theta},$$

where N is a multiple of the power line frequency, J is the moment of inertia of the armature plus the rotor, ε is the phase error, K is the stiffness coefficient of the system, and θ is the power line phase angle. In the limit of Butterworth damping, $C = \sqrt{2KNJ}$, one can show that the power spectral density of the phase-lag error is given by

$$(3)\quad \frac{d\Upsilon^2}{d\nu} = \left(\frac{T}{2\pi\nu_0}\right)^2 \frac{(\nu/\nu_0)^2}{1+(\nu/\nu_0)} \frac{d\sigma^2}{d\nu} \quad .$$

Here T is the period and $\nu_0 = (2)^{-1}\sqrt{K/NJ}$. For $\nu_1 << \nu_0$, one can then show that the RMS phase-lag error is

$$(4)\quad \Upsilon_{RMS} = \frac{2\pi\sqrt{2}\,NJ}{F_0 K}\,\sigma_1\nu_1$$

and the RMS control power is

$$(5)\quad P_{RMS} = 8\pi^3\sqrt{2}N^2F_0J\sigma_1\nu_1 \quad .$$

The available power must be must greater than (5) to keep the control system linear. If one estimates ten times (5), then, for a typical rotor of J = 500 $kgcm^2$ operating at 32,400 RPM, one obtains a control power requirement of 230 W. Additional power is required to overcome bearing drag.

III. Control System for 14,400 RPM Test

A PID control system was tested using one of the choppers from the MTR velocity selector[2]. Fig. 4 shows the control system in schematic form.

The input signal E_L is the train of 20 μsec pulses of 120 Hz nominal repetition rate, corresponding to the successive zero crossings of the powerline voltage waveform. The output is the advancing phase angle θ of the chopper shaft S, which rotates at the nominal speed of 2 X 120 = 240 Hz. Each revolution of the shaft is detected by a magnetic pickup Q which senses the passage of a slot in the iron disk D attached coaxially to the shaft (or equivalently an iron stud attached to the chopper rotor). The signal conditioner P squares up the rough pulse train from the pickup Q, and delivers (as a feedback signal E_R) a train of 20 μsec pulses of 120 Hz normal repetition rate.

The shaft S is driven by a 500 W, 2 phase, 4 pole induction motor M, which receives its stator excitation from a 2 phase, 240 ± 48 Hz, variable-frequency drive unit. Each phase of the drive unit is a 250 W solid state amplifier, connected to an 8-bit digital-to-analog converter which has its data input furnished by a 256-byte read-only-memory ROM. The phase one memory contains a cosine wave, and the phase-two memory contains a sine wave. The two ROM's are addressed simultaneously by the parallel outputs of an 8-bit binary counter, which is toggled by a voltage-controlled oscillator having a 61.4 $\pm$ 12.3 kHz output frequency which is linearly related to the input voltage V.

The function of the controller box B is to transform the line signal E_L and the rotor signal E_R into a control voltage V which will maintain phase lock within an acceptable phase tracking error. Early studies showed that the conventional rate generator in a standard PID controller is far too insensitive to detect the miniscule, but crucial, speed changes. Instead, a digital timing-and-computing scheme was devised to measure the relative phase lag and the duration of every revolution of the shaft S with an accuracy of $\pm$ 204 nsec, and to convert the resulting data streams into a phase error signal and "vernier speed error" signal needed to stabilize the associated phase loop.

In obtaining the experimental data reported here, the speed error gain setting was such that full scale correction ($-10 < V < +10$ volts) corresponded to a ± 0.375 Hz speed error. The phase error gain was manually set to the highest value achievable without inducing overshoot oscillations. With the motor and chopper running in a one Torr vacuum, the four supporting bearings consumed an average drag power of $\sim$150 W.

IV. Phasing Experience

As a test of the PID control system, one of the surplused choppers from the MTR velocity selector[2] was reactivated. This chopper has a moment of inertia of about 200 $Kgcm^2$. The 500 W

motor was used to drive the chopper at speeds up to 14,400 RPM. A magnetic pickup was used to sense an iron stud on the chopper to record the chopper's relative angular position. Figure 5, which demonstrates the phase control, shows the spectrum of magnetic pickup events when the chopper is controlled to the line and the scan is triggered by the time of the zero crossing signal from LAMPF. The full width half maximum FWHM of this curve is 15 μsec, while the full width at the base FWB is 45 μsec. These times are both well within the window of 128 μsec in which LAMPF will allow for a trigger from the chopper to be sent back to trigger LAMPF.

Figure 6, which is a first demonstration of the jitter, shows the spectrum of magnetic pickup events when the chopper is controlled to the line and LAMPF is triggered by the chopper. The FWHM is 2.0 μsec while the FWB is 5.0 μsec, both approaching the conditions that will be satisfactory for a phased chopper.

Since the MTR chopper with its Ni shell and Ni + Cd shades in the foil package will not be satisfactory for chopping neutrons above 0.3 eV, a new chopper was made. This new chopper, which is shown in Figure 7, has a shell of Al and shades in the foil package of three pieces of Borsical[9,10], a composite of B fiber covered with Al. The radius of curvature of these slots is 130" to pass 0.5 eV neutrons when the chopper is spinning at 14,400 RPM. The moment of inertia of this chopper is 100 $Kgcm^2$.

Figure 8 shows an example of the phase control for the Al shell chopper while Figure 9 shows the jitter. The chopper was spinning at 14,400 RPM. Figure 8 shows that the control or phase lock of the chopper to the line that drives LAMPF was 50 μsec FWB, well within the 128 μsec window allowed by LAMPF. Figure 9 has a FWHM of 1.8 μsec and a FWB of 6 μsec, close but not as narrow as desired. Analysis of parts of the control system indicate that the adjustable delay #1 of Figure 1 has a jitter of ± 1 μsec while the adjustable delay #2 has a jitter of ± 0.5 μsec. These could account for much of the ± 1 μsec jitter of Figure 9. Inspection using an oscilloscope of the change in speed of the chopper as sensed by the magnetic

pickup signal indicates a short time jitter of only a few tenths of a μsec. This should represent the jitter that is achievable with the PID control system when the coarseness of the delay units is reduced.

A longer time hunting is observed in the speed of the chopper. This may cause some jitter and a longer time-integral control may need to be used in the control system.

IV. Neutron Experience

For neutron tests, the Al shelled chopper was placed at flight path 8 of WNR. A fluted beam was used which viewed the 10cm X 10cm source at the target through a 2cm X 0.13cm slot at the chopper. Neutron detectors were placed just before the chopper, and just after the chopper.

Figure 10 shows spectra of the flux of neutrons that were measured by the two detectors. The upper curve of Figure 10 is the typical WNR spectrum for a beam filtered only by Cd. The increase near channel 600 is the start of the thermal Maxwellian distribution. The dip near channel 900 indicates the Cd cut off. The lower curve of Figure 10 shows the bursts as sensed by the detector just after the chopper, for several different phase settings. Since the detector was near the chopper and in a high field of scattered neutrons, the backgrounds of the lower curve are not indicative of the true effectiveness of the chopper when closed. The envelope of the bursts of the lower curve show the coarse transmission of the chopper.

The bursts are sharp, even the first burst at channel 60 which is about 20 eV. The 4th burst is at about 0.4 eV, a little below the design target for maximum transmission for this chopper. The last burst at channel 950 is for about 80 meV neutrons which are so slow that they are mostly swept out by the nearly straight slots.

Figure 11 shows an expanded view of the 4th burst, the one for 0.4 eV neutrons. Its FWHM which is 10 μsec, is a composite of the 5.2 μsec FWHM of the chopper opening and closing, the 11.2 μsec FWB of the sweep of the chopper across the source and the 2 μsec FWHM of

the jitter of the chopper. The boron shades made of three thicknesses of Borsical seem to be effective for chopping neutrons even up to 20 eV. The background of Figure 11 is not significant because of the way these tests were run.

V. Conclusions

The control tests and neutronic tests presented in this paper demonstrate that the PID control system effectively holds a chopper within the time window allowed by LAMPF. The jitter measurements show that a chopper can trigger LAMPF to within $< \pm 0.5$ μsec once the electronic coarseness is refined. The neutronics measurements show that the boron fiber shades are effective neutron choppers.

Acknowledgements

The authors recognize and thank Harold Bowen for his many contributions and assistance in the construction and checkout of the PID control system. Rod Hardee was a great help in reassembling the MTR chopper. The authors also thank Joyce Goldstone, Phil Seeger and Don Crocker for valuable assistance during the course of this development.

References

1. R. A. Egelstaff, "Proceedings of the First International Conference on the Peaceful Uses of Atomic Energy", Geneve, Vol IV, p. 119, United Nations, New York, (1955).

2. R.M. Brugger and J.E. Evans, Nuclear Inst. and Meth., 12, 75, (1961).

3. W. D. Whittemore and H. R. Danner, "Neutron Inelastic Scattering," Vol 1, p. 273, IAEA, Vienna, (1963).

4. G. J. Kirouac, W. E. Moore, L. J. Esch, K. W. Seeman and M. L. Yeater. Thermalization of Reactor Spectra Vol 1, p. 389, IAEA, Vienna, (1968).

5. B. C. Boland, D. F. R. Mildner, G. C. Sterling, L. J. Bunce, R. N. Sinclair and C. G. Windsor, Nucl. Inst. and Meth. 154 349, (1978).

6. R. Kleb, C. A. Pelizzari and J. M. Carpenter, "Fermi Choppers for Epithermal Neutrons", (in preparation).

7. C. G. Windsor, Pulsed Neutron Scattering, pp. 296, Taylor and Francis LTD, London, (1981).

8. T. J. L. Jones and J. G. Parker, Proceedings of the IVth ICANS Meeting, KEK, TSUKUBA, Oct 20-24, (1980), KENS Report II, pp 499, (March 1981).

9. Composite Technology, Inc., 6 Mill Street, Broadbrook, Conn. 06016.

10. T. J. L. Jones, J. Penfold and W. G. Williams, Rutherford Laboratory Report RL-79-020, (March 1979).

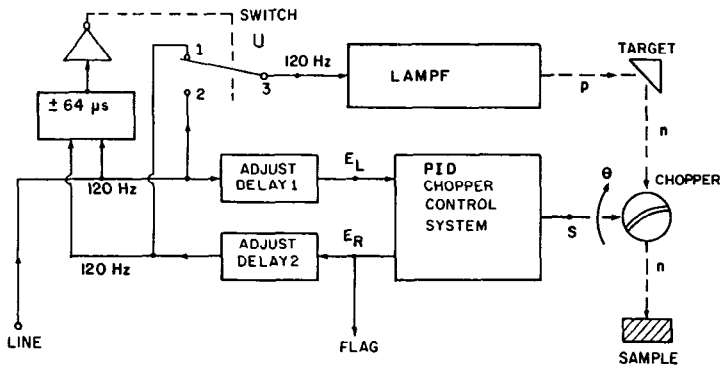

Fig. 1

Schematic layout of the coupling of a chopper at WNR to the LAMPF accelerator.

Fig. 2

Period deviation from 60 Hz versus time of the LAMPF commercial power line.

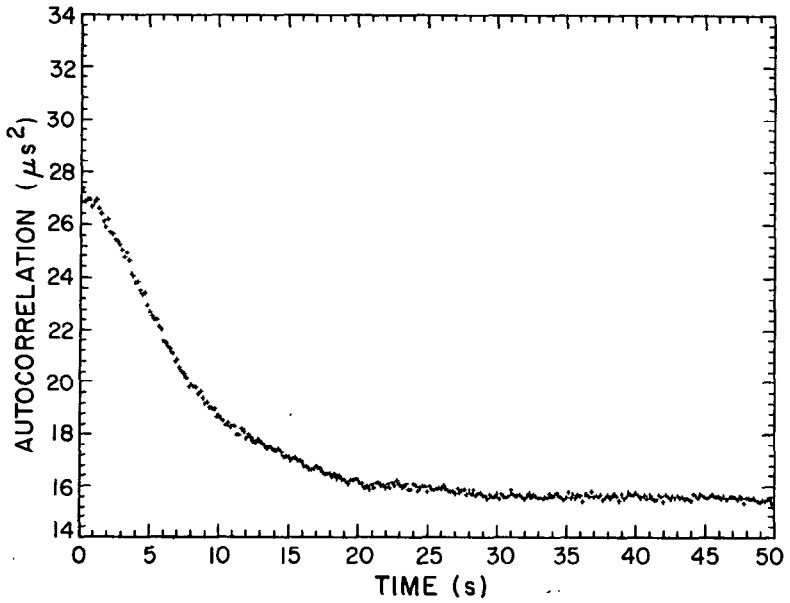

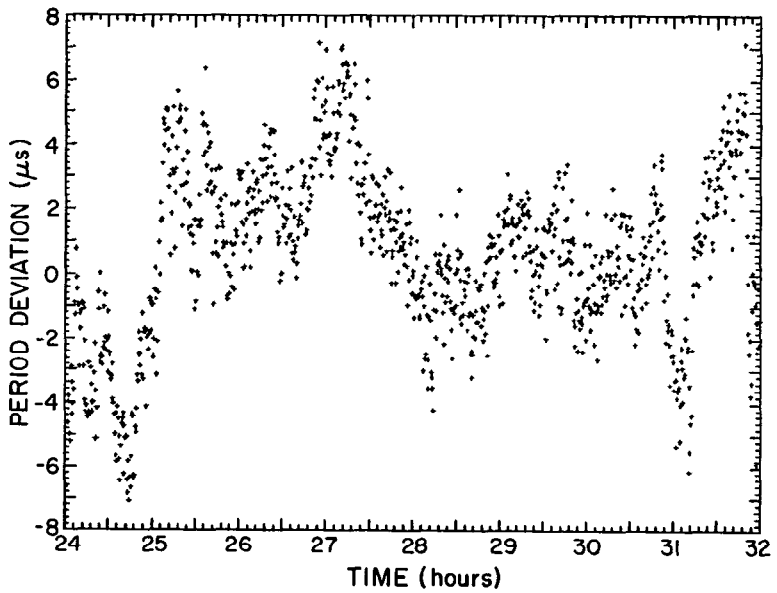

Fig. 3

Autocorrelation of the period deviations of Figure 2.

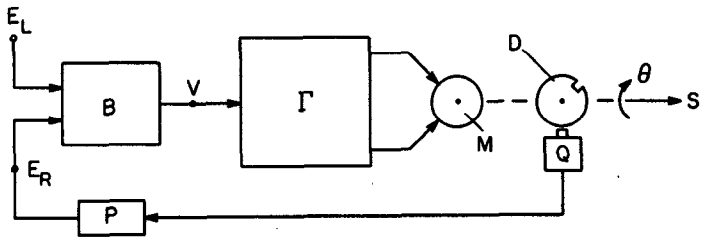

Fig. 4

The neutron chopper control system.

Fig. 5

The measured phase error distribution between the LAMPF power-line cross-over and the chopper angular position using the PID control system. The chopper had a nickel shell, a moment of inertia of 200 Kgcm^2 and was running at 14,400 RPM.

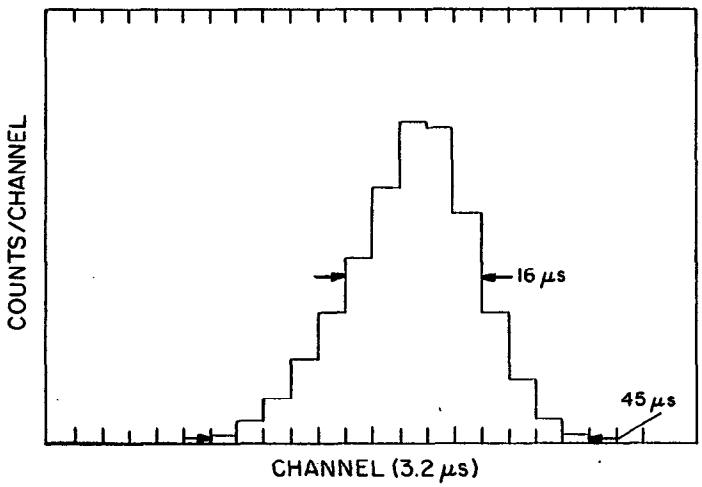

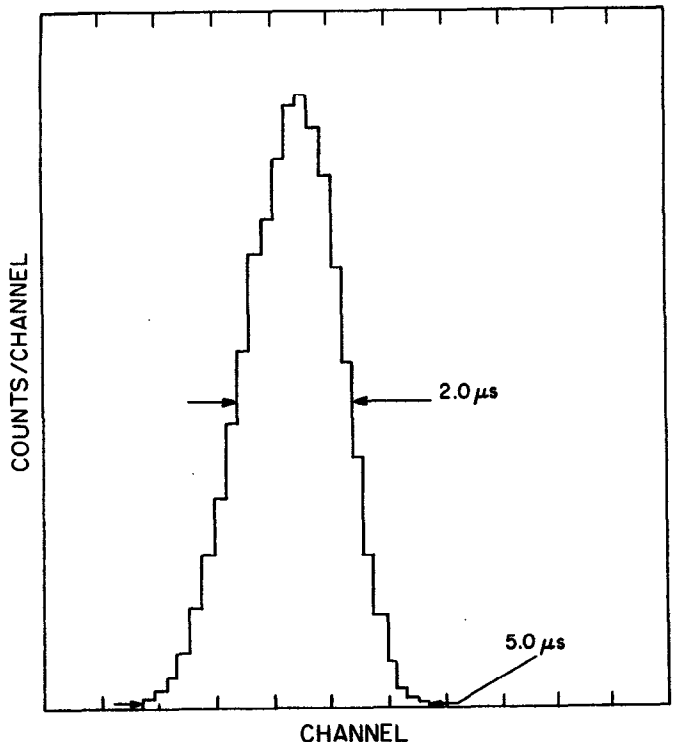

Fig. 6

The chopper jitter distribution when the chopper is phased to LAMPF as in Figure 5 and LAMPF is fired within the 128 μsec window. In this case, the chopper was spinning at 7,200 RPM.

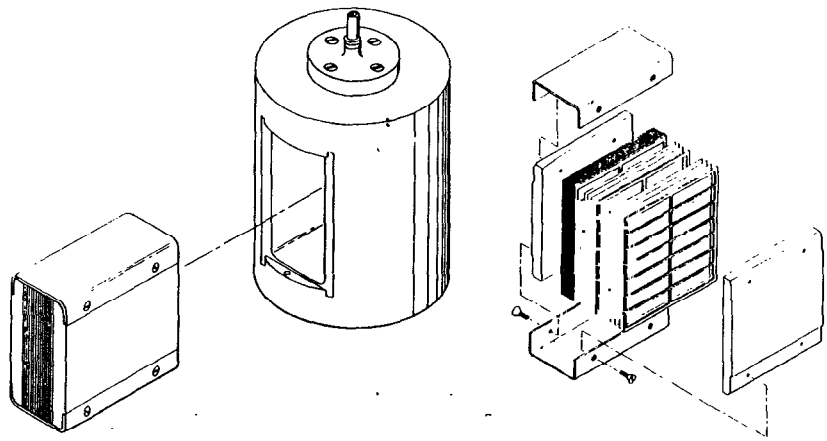

Fig. 7. A drawing of the Al shell chopper with the Al shell in the center, a foil package to the left and an exploded view of the foil package to the right.

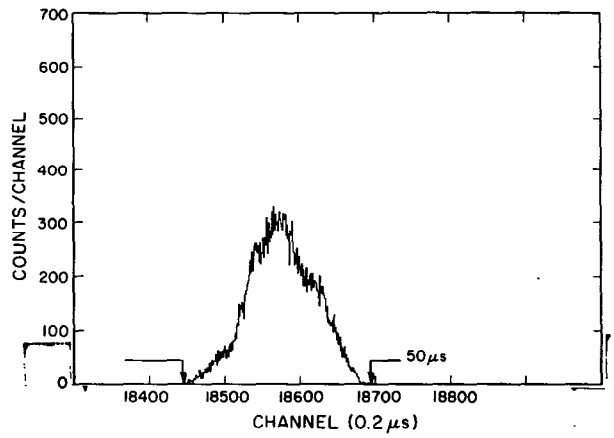

Fig. 8. The control or phase error distribution for the Al shell chopper with 100 Kgcm^2 spinning at 14,400 RPM.

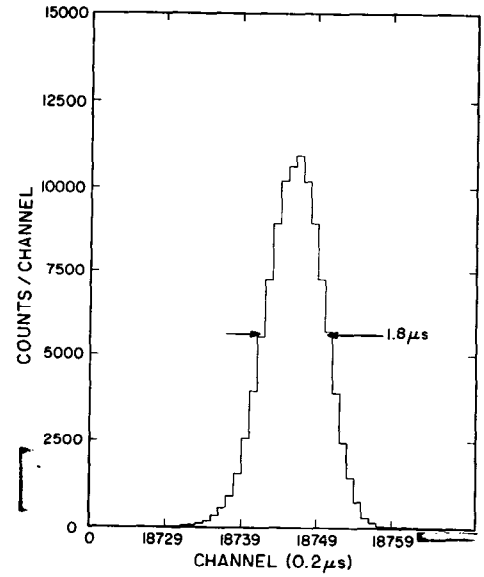

Fig. 9. The chopper jitter distribution with the Al shell chopper phased to LAMPF as in Figure 8 and LAMPF being fired by the chopper. The chopper was spinning at 14,400 RPM.

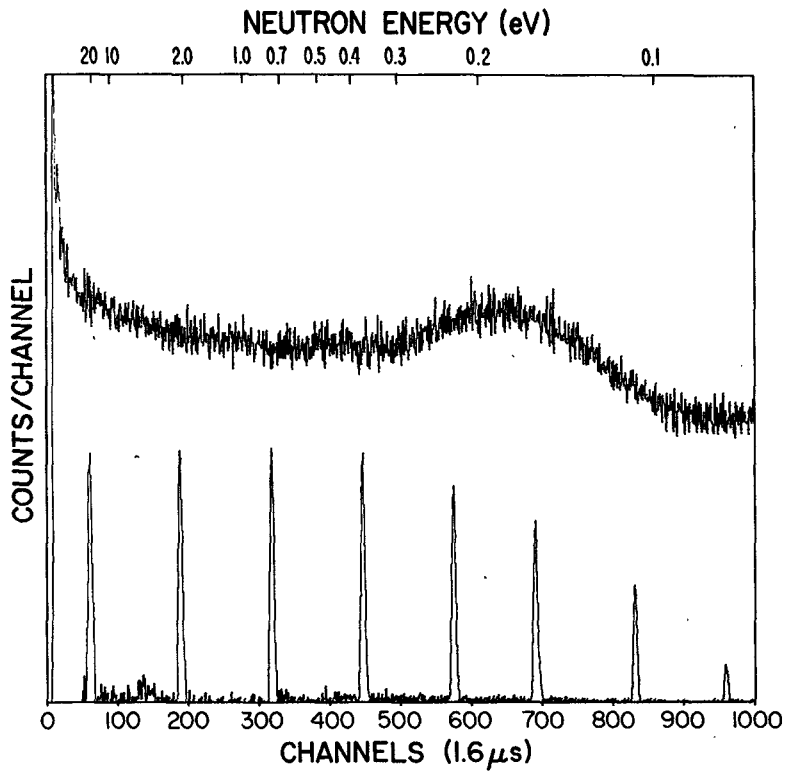

Fig. 10. Spectra of the flux of neutrons measured in flight path 8 by detectors just before and just after the chopper.

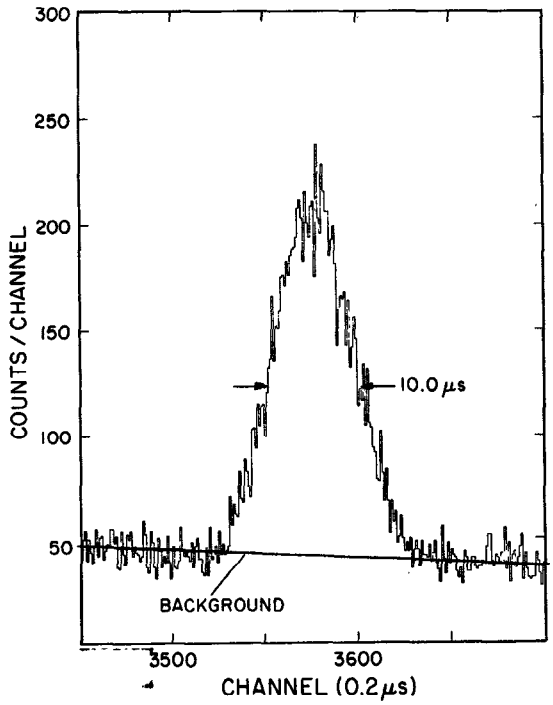

Fig. 11

An expanded view of the 4th burst from the left of Figure 10.